TM-1176
8055.000

A DESIGN FOR ANTIPROTON COLLECTION AND BEAM TRANSPORT IN THE FERMILAB TEVATRON I PROJECT*

E. Colton+, and C. Hojvat

March 1983

* Presented at the 1983 Particle Accelerator Conference, Santa Fe New Mexico, March 21-24.
+ Argonne National Laboratory

A DESIGN FOR ANTIPROTON COLLECTION AND BEAM TRANSPORT IN THE FERMILAB TEVATRON I PROJECT

Eugene Colton+
Argonne National Laboratory†

and

Carlos Hojvat
Fermi National Accelerator Laboratory*
P.O. Box 500, Batavia, IL 60510.

Summary

120 GeV protons from the Main Ring will be used to produce 8 GeV antiprotons. A pulsed lithium lens collects and matches the antiprotons to a beam line for injection into the Debuncher Ring. The $\bar{p}$ beam has a transverse emittance of 20π mm-mr and a $\delta p/p = \pm 2.0\%$. The beam line consists of a clean-up section with vertical emittance selection, two long dispersion free sections, a bend and a vertical injector. Antiprotons with a transverse emittance of 2π mm-mr and $\delta p/p = \pm 7.0 \times 10^{-4}$ are transported in the reverse direction, bypassing the target area, and along the 120 GeV proton transport line for reverse injection in the Main ring.

Introduction

The Tevatron I project will provide colliding beams of protons (p) and antiprotons ($\bar{p}$) for high energy physics experiments.[1] The $\bar{p}$ are produced by 120 GeV protons. Antiprotons of 8 GeV kinetic energy are collected with a lithium lens and transported to a large acceptance ring, the Debuncher. After phase rotation, the $\bar{p}$ bunches are transfered into the Accumulator ring for cooling and accumulation. Part of the cooled stack is extracted from the Accumulator, transported and reverse injected into the Main Ring for subsequent acceleration to 1 TeV. We discuss a first design for: i) $\bar{p}$ collection and transport to the Debuncher, and ii) $\bar{p}$ extraction and transport to the Main Ring.

Figure 1 shows the overall geometry of the p source with the transport lines and other accelerators at Fermilab.

As the design of the Antiproton Source evolves, we expect the beam transport systems to undergo changes to account for geometry changes and variations in the design of the Debuncher and Accumulator rings. The beams here described correspond to the designs of Reference 1.

Antiproton Collection

A pulsed lithium lens follows the target. Its characteristics have been extensively described elsewhere.[2] The device functions as a cylindrically symmetric focussing thick lens, with dimensions 15 cm long, a 1 cm radius and a focusing gradient of 1000 T/m. The focal length is 22.5 cm (f^*=14.5 cm) for 8 GeV $\bar{p}$. We have compared the relative performance of this $\bar{p}$ collection scheme to that of a conventional quadrupole triplet or pulsed quadrupole multiplet.

The lithium lens is more efficient in the collection of beams of large transverse emittance and $\delta p/p$, even when multiple scattering and absorption is included.[3]

The lithium lens collects the beam following a source of effective $\beta^* = 0.0225$ m with maximum 60 mrad divergence and $\delta p/p = \pm 2.0\%$. The chromatic aberrations of this system are extremely small due to the short focal length of the lens -even at +2 or -2% we find a 94% efficiency.

Antiproton Transport to Debuncher

The target to Debuncher line shown in Figure 1 must be capable of selection of maximum emittance up to 20π mm-mr and maximum $\delta p/p$ up to ±2%.

The first part of the beam is a clean-up section composed of a pulsed dipole which bends 8.89 GeV/c negative secondaries 3° left (positives to the right and into a dump), two quadrupole doublets and another 3° bend in order to complete the achromatic transformation. Charge, central momentum and vertical emittance are selected within this section using collimators.

The second and fourth parts of the beam consist of three 90° FODO quadrupole cells and matching lenses. The periodic structure has a cell length of 27.1 m with β_{max}/β_{min} = 45.9 m/ 7.98 m. The third beam section consists of six dipoles and four quadrupoles. This section serves to: i) bend 36.53° left to establish beam direction to the Debuncher; ii) horizontal emittance selection at the entrance and exit where $\beta_x^* = 80$ m; iii) fine $\delta p/p$ selection in the centre of the bend section where $\beta_x^* = 5.0$ m and a maximum in the dispersion $|\eta_x^*| = 2.62$ m is obtained. The first order momentum resolving power for $\delta p/p = 1\%$ is $R = 10\,|\eta_x^*|/2\sqrt{\beta_x^* \varepsilon_x/\pi}$ with R = 1.31 for $\varepsilon_x = 20\pi$ mm-mr. The fourth section is composed of quadrupoles, its length dictated by the positioning of the Debuncher and Accumulator rings. The final section is an achromatic vertical translation bringing the beam down to the Debuncher ring level.

The beam was designed using the program TRANSPORT.[4] Figure 2 shows the monoenergetic β_x, β_y envelope functions and the beam dispersions η_x and η_y from the target to the Debuncher injection area.

Control of the injected beam relative momentum spread is important for tuneup of the Debuncher. Horizontal slits, at positions $\pm x_s$, located at the centre of the left bend, allow $\delta p/p$ selection. The program TRANSPORT was used to predict the horizontal beam distributions at the centre. For initial coordinates $x=x_o$(mm), $x'=x_o'$(mr) and $\delta p/p$ (%) the value is given by:

+ Now at Los Alamos National Laboratory.

† Operated for the U.S. Department of Energy by the University of Chicago.

* Operated by the Universities Research Association, Inc., under contract with the U.S. Department of Energy.

$$x_c = -0.141\, x_o + 0.335\, x_o' - 26.2\, \delta p/p + (4.65\, x_o - 0.177\, x_o' + 0.48\, \delta p/p)\, \delta p/p$$

Sets of rays at two vaues of $\delta p/p$, uniformly distributed in $x_o - x_o'$ space were generated, for both $\epsilon = 5\pi$ mm-mr and 20π mm-mr for the initial $\beta^* = 2.25$ cm. The fractions of rays having $|x_c| < x_s$ is shown in Figure 3. Each curve represents a different slit opening. Figure 3 indicates that for an emittance of 5π we can pass a band in $\delta p/p$ of $\pm 0.2\%$ for $x_s = \pm 5$mm, with full transmission of the monoenergetic rays.

Chromatic aberrations of the transport line further degrade the efficiency of the $\bar{p}$ beam match to the Debuncher. Calculation of this efficiency is very sensitive to the lattice parameters at injection. Changes in these parameters will affect the conclusions below. The effect was studied by ray tracing of 5000 particles generated in transverse phase space according to a "water bag" distribution, at each value of $\delta p/p$. Figure 4(a) shows the fraction of rays at each $\delta p/p$ falling within the admittances of the Debuncher in both planes. The efficiency drops to 50% at $\pm 2.0\%$, but with an integrated efficiency of 80% over the whole range. Figure 4(b) shows the expected ratios of the final to initial rms emittances as a function of $\delta p/p$. The vertical plane exhibits a somewhat larger emittance growth.

Antiproton Transport to Main Ring

Figure 1 also shows the location of the beam line for the cooled $\bar{p}$ beam. The expected characteristics are $\epsilon = 2.0\pi$ mm-mr and $\delta p/p = \pm 7.0 \times 10^{-4}$. Vertical extraction from the Accumulator is followed by a standard achromatic translation system that restores the extracted beam to target elevation (+48" above ring level). The beam is then taken through four sections: i) long transport, ii) left bend, iii) long transport and iv) target bypass. Following the bypass the beam rejoins the 120 GeV proton line for reverse injection into the Main Ring.

The long transport uses quadrupoles in a 90° FODO channel with matching lenses. The periodic structure has a cell length of 50.8 m with β_{max}/β_{min} = 86.6 m/ 14.9 m.

The left bend is performed using three dipoles for 18.62° left. The long transport (iii) runs parallel to the $\bar{p}$ beam into the Debuncher. The target bypass is an achromatic transport using three dipoles and three quadrupoles. The third dipole is energized to direct the $\bar{p}$ beam in the direction of the 120 GeV beam line. Figure 5 shows the behavior of the monoenergetic beam functions β_y, β_x, η_y and η_x through the system, as calculated with TRANSPORT*

Acknowledgements

Special thanks are due to the Tevatron I staff, especially to A. Ruggiero and D. E. Johnson for many usefull discussions.

References

1."Design Report Tevatron I Project", Fermilab, October 1982.

2."Mechanical and Electrical Design of the Fermilab Lithium Lens and Transformer System", G. Dugan et. al., this conference.

3."More on Antiproton Collectors", E. Colton, Fermilab $\bar{p}$ note 120, March 1981.

4."TRANSPORT", K.L. Brown et. al., CERN 73-16 (1973).

Figure Captions

Figure 1.- Plan view of the antiproton transport lines with reference to the Fermilab site.

Figure 2.- Monoenergetic beam functions for the $\bar{p}$ transport from the target to the injection into the Debuncher.

Figure 3.- Fraction of beam transmitted at the momentum collimator vs. $\delta p/p$ for two different beam emittances and for the indicated slits opening.

Figure 4.- (a) Transport efficiency of the p beam into the Debuncher admittance for $\epsilon = 20\pi$ mm-mr vs. $\delta p/p$. (b) Growth factors in rms emittance after $\bar{p}$ transport into the Debuncher.

Figure 5.- Monoenergetic beam functions for the $\bar{p}$ transport from the Accumulator extraction to the match point in the 120 GeV line.

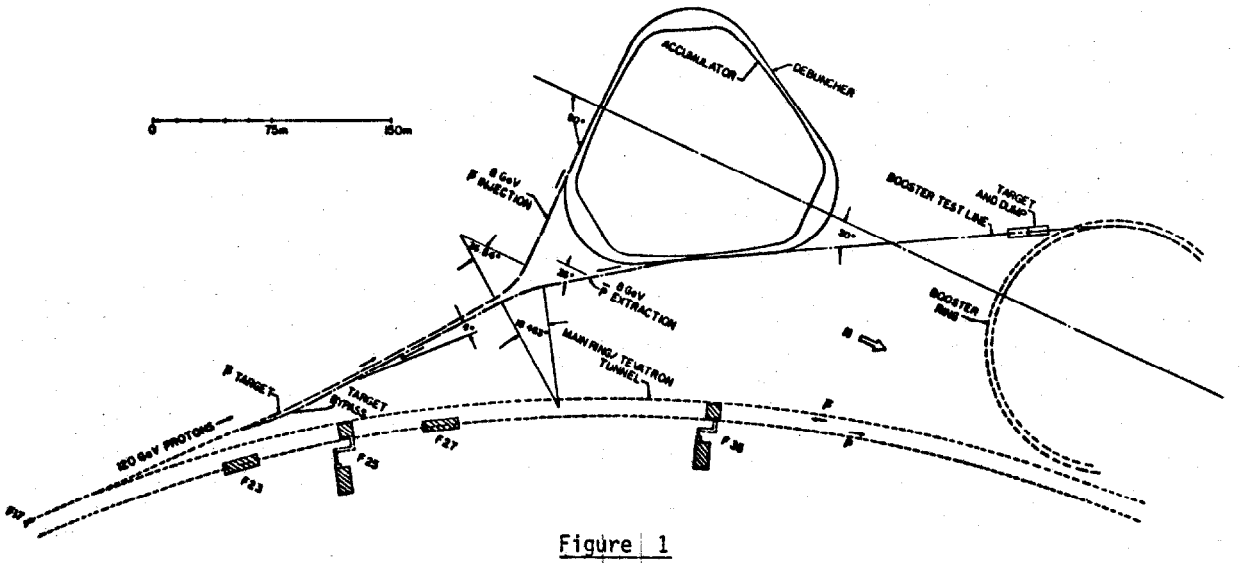

Figure 1

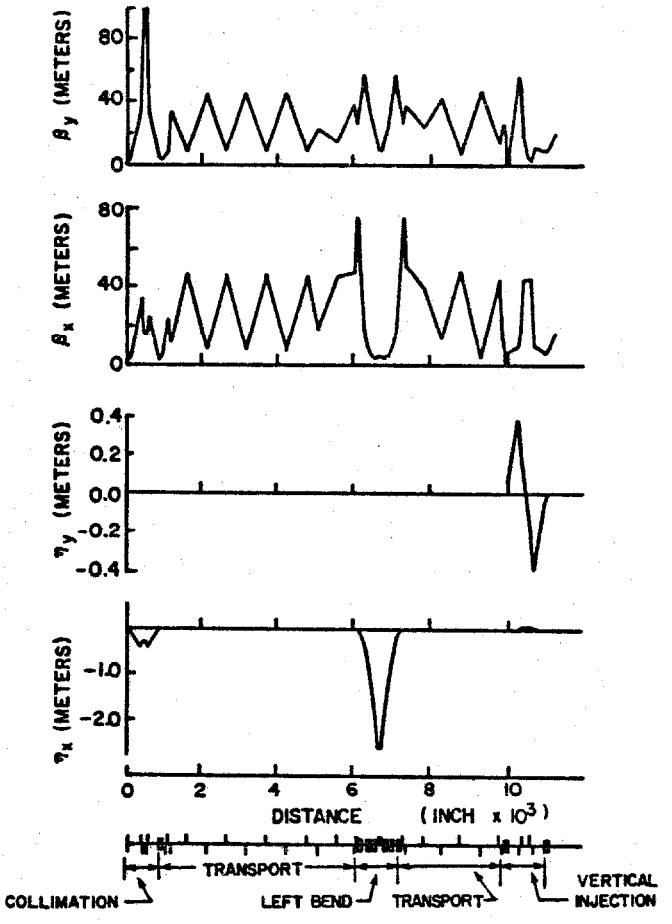

Figure 2

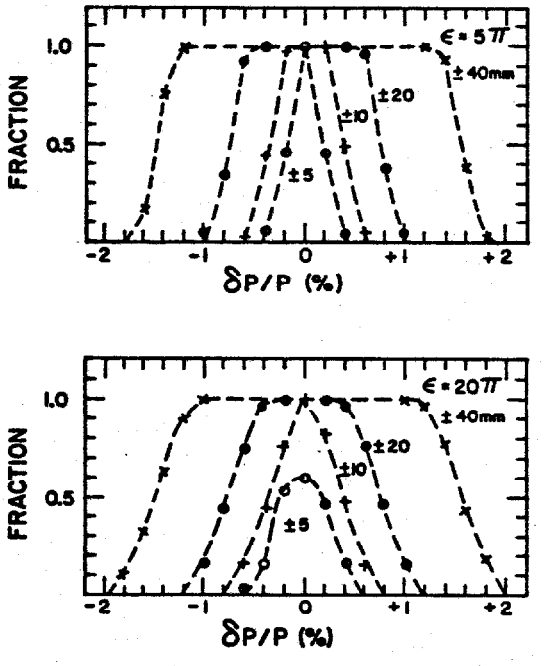

Figure 3

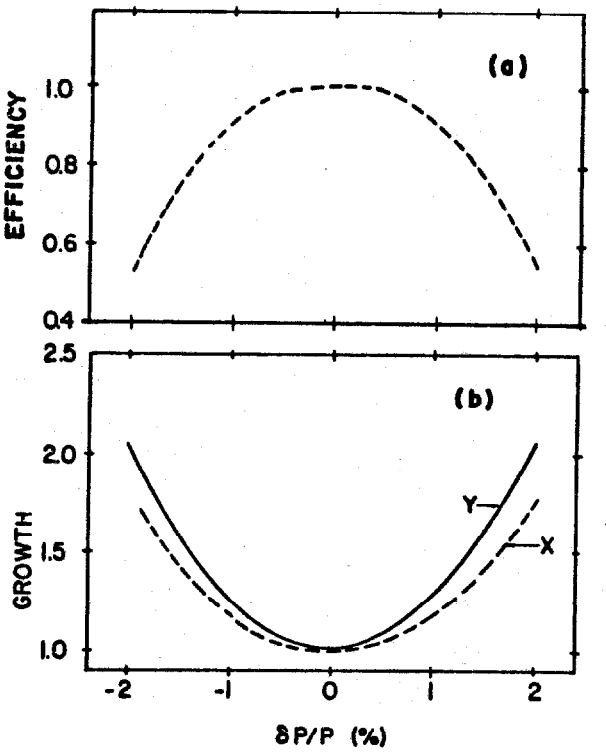

Figure 4

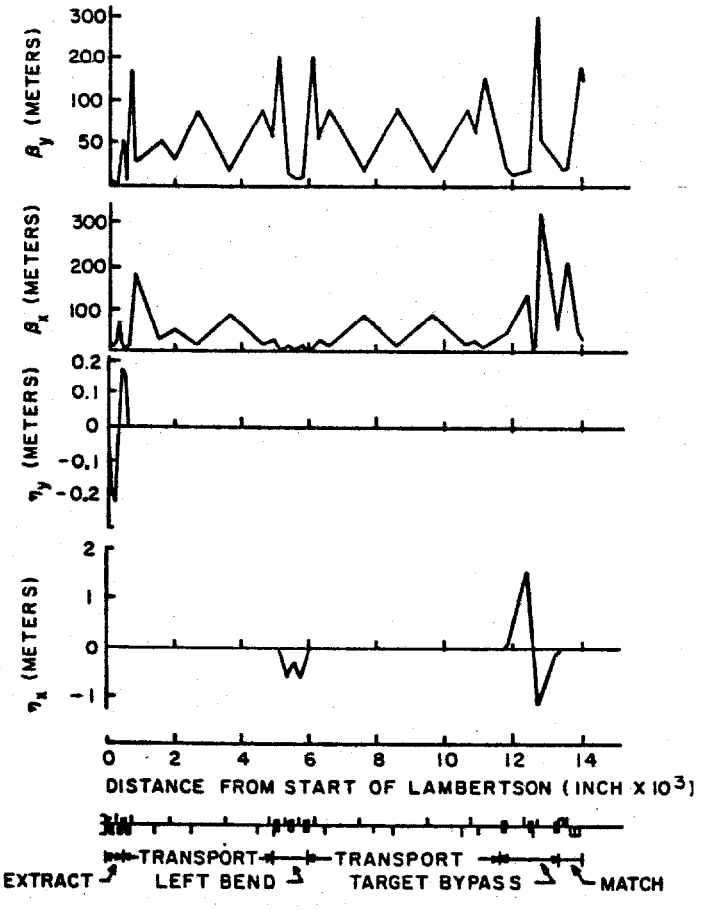

Figure 5